Shahrood University of Technology

Journal of Mining and Environment (JME)

Journal homepage: www.jme.shahroodut.ac.ir

Iranian Society of Mining Engineering (IRSME)

Stability Assessment of Stopping Operations in Friable Ore Bodies under an Open Pit Mine using Strength-based Mining Sequence Factor

Sruti Narwal[1]*, Debasis Deb[1], Sreenivasa Rao Islavath[1], and Gopinath Samanta[2]

1. Mining Engineering Department, Indian Institute of Technology, Kharagpur, India
2. Senior Technologist (Mining), Process Technology Group, Tata Steel Limited, Jamshedpur, India

Article Info

Received 2 August 2024
Received in Revised form 29 November 2024
Accepted 6 December 2024
Published online 6 December 2024

DOI: 10.22044/jme.2024.14872.2828

Keywords

Friable ore and host rocks
Mining under open pit
Novel mining method
Stope and pillar system
Mining sequence factor

Abstract

A novel underground mining method is proposed to extract friable chromite ore bodies in weak and weathered limonitic host rock below an open-pit mine. The conventional underground methods do not instill confidence since GSI (Geological Strength Index) of ore bodies and host rock lies below 35. Series of dimensions of transverse stopes along the strike are suggested based on a detailed analysis of multiple mining and backfilling operations by simulating 36 three-dimensional numerical models. For each operation or sequence, a strength-based "Mining Sequence Factor (MSF)" is devised that helps quantifying its equivalent strength compared to in-situ conditions. This factor along with the Average Equivalent Plastic Strain (AEPS) developed on the pillars as obtained from numerical models is used to determine the safe operations with desired yearly production target. The paper provides an in-depth analysis of this method and suggests minimum pillar dimensions of 40 m, whether in-situ or backfilled. The paper, in addition, lays the design of underground drives and their support system as per NGI (Norwegian Geotechnical Institute) guidelines and 3D numerical studies, the performance of which is analysed considering distribution of stress and equivalent plastic strain.

1. Introduction

An open-pit chromite mine is being operated in a valley having weak and weathered sedimentary deposits rich in limonitic mineral as the host rock. Two ore bodies, Middle Band (MB) and North Band (NB), each with a dip of 85º, and a thickness ranging from 15 m to 25 m are extracted with shovel and dumpers. The plan view of the studied site is shown in Figure 1a, where the red box encloses the open-pit area under study. A sectional view of the ore bodies and host rocks at latitude E 3100 is depicted in Figure 1b. The Ultimate Pit Limit (UPL) is designed at a depth of 15 m RL (marked as UPL1) for MB and -10 mRL (marked as UPL2) for NB. Further adding to the complications, the ore bodies are also friable in nature, having an average uniaxial compressive strength between 1200 kPa and 2000 kPa. Blasting is required to fracture ore bodies, only wherever they are found to be lumpy and hard. The compressive strength of the limonitic rock (marked as HR1 in Figure 1b) is between 700 kPa and 900 kPa, and naturally, no blasting is required for their removal from the overburden benches. The geotechnical and geological explorations have established that the friable ore bodies exist beyond the pit limit up to -130 mRL depth, after which, they gradually harden and attain over a 100 MPa strength at a depth between -150 mRL and -170 mRL (this transition is marked in Figure 1b). The host rock follows a similar trend as the ore body, and it changes from limonitic rock to hard and strong serpentinite (marked as HR3 in Figure 1b, while the transition between HR1 and HR3 is marked as HR2, also referred to as a weak

Corresponding author: srutinarwal27@gmail.com (S. Narwal)

serpentinite) as the depth increases. Similar to the division of host rocks as HR1, HR2, and HR3, the ore bodies are also divided. The field investigations on rock mass quality suggests Geological Strength Index (GSI) is between 25 and 35 for both the host rock and ore bodies, having mostly blocky to disintegrated pieces and weathered surfaces. It is estimated that the stand-up time of such rocks is below one hour, and any delay in supporting can result in a collapse of the structure.

Soltani with Osanlo [1] determined the optimal interface between the open-pit and underground mining methods for extracting coal seams gently dipping at 20-30˚. They found the ultimate open-pit limit to not more than 200 m below the ground surface. On the other hand, when a surface mine reaches its ultimate depth, the mine often transitions to underground leaving a certain thickness of the ore body at the bottom of the open pit, called "crown pillar" [2-4]. In some cases, a natural crown pillar may also be replaced with an artificial one if the wall rocks are competent, and the grade of the ore body is high, which enables full recovery of the natural crown pillar [5]. Disappointingly, in the present study, because the strength of both the ore and host rocks is low, it would require a much thicker crown pillar (over 100 m is the depth until the wall rocks are expected to be competent), resulting in a permanent loss of the high-grade chromite ore.

The Nicholas [6] and Hartman [7] method classification systems are also traditionally used to select a suitable mining method for a given geo-mining condition. Over time, as the importance of key selection has grown, the multi-criteria decision-making methods have been employed to meet this need. Dehghani [8] applied grey and TODIM (Portuguese acronym for Tomada de Decisão Interativa Multi-critério) models to determine the best method for iron ore extraction, and concluded that the open-pit mining method is the most appropriate choice, while the square-set mining is the worst one. Alpay and Yavuz [9] also provided a decision support system to select an underground mining method. Similarly, in the context of selecting underground mining methods, the use of fuzzy set theory was explored [10- 11], Analytic Hierarchy Process (AHP) was applied to identify the most appropriate method for an underground mine [12-15].

In case of the given open-pit chromite mine, which has reached its ultimate pit limit, following the assessment based on the Nicholas and Hartman methods, cut and fill Stopping (Nicholas score of 38) and square-set Stopping (Nicholas score of 41) arrive to be the closest possible solutions, but seem redundant when it comes to capital investment as well as safety measures. For example, square-set Stopping relies on creating large, open stopes, which are supported but may not adequately ensure the stability of friable materials prone to crumbling or disintegration, and may rather destabilise friable rock formations to an extent of collapse. Secondly, the cut and fill Stopping method does involve ore removal in small increments, and subsequent filling of the voids, thereby, reducing the risk of collapses but ensuring stability of wide exposed roof and efficacy of bolting in such rocks is a question mark. The method also requires leaving behind a thick crown pillar. The other suggested methods are the caving methods that will cause extensive ore dilution as well as obviously, jeopardise the stability of the open-pit benches, in a case where the stability of the benches is of prime concern to the management. Not only are the conventional mining methods unfavourable, literature suggests no instances of extracting ores from such weak, fractured, and friable formations. Most of the stope designs either involve competent host rocks with poor or fair ore bodies or vice versa. An open-pit mine transitioned to underground with ores stronger than 100 MPa and host rocks at 12-140 MPa [16]. Another open-stope design was proposed for a mine with rocks having GSI > 60 [17], and in another gold mine with a 50 m crown pillar [18]; one example is found where caving induced in competent host rocks from the previous underground methods, and it was later decided for a single top-down sequence [19].

In fact, the mine management has a plan to mine the hard portion of the ore body by the conventional underground mining method, leaving a crown pillar of 100 m, but no method gives confidence for extracting the friable ore bodies below the UPL. This left the management with no choice but to leave the friable ore bodies in the ground. However, given the huge economic value of the high-grade chromite within these formations and in line with sound mining practices, this geotechnical project has a pressing need to come up with a fresh research idea for extracting these resources. Interestingly, it is also observed that, despite several seasonal rains, overburden benches have remained in situ, and visibly appear stable and intact.

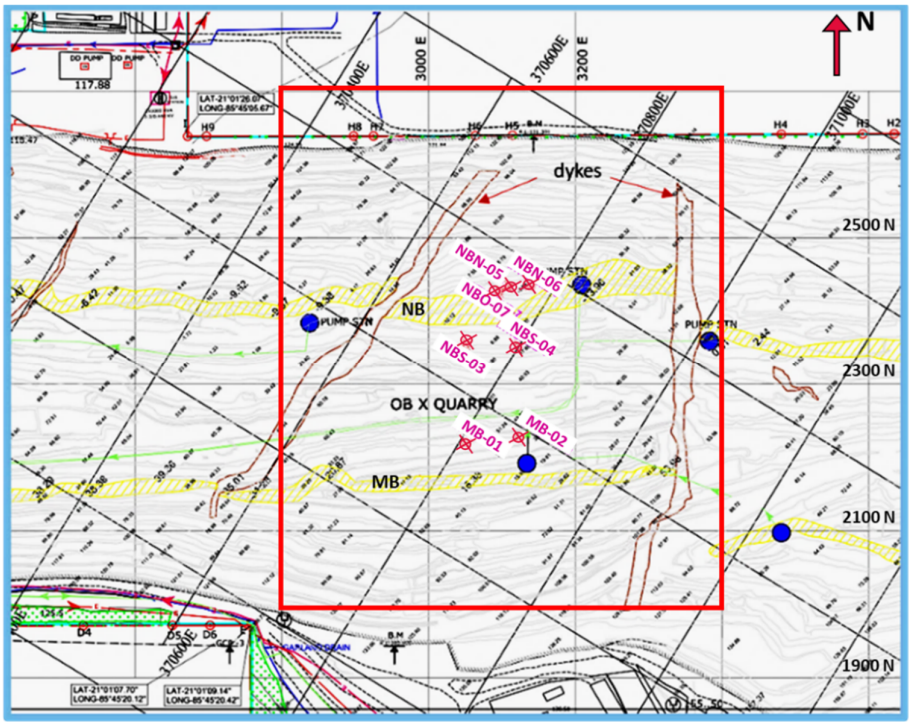

a) Plan view of the studied site.

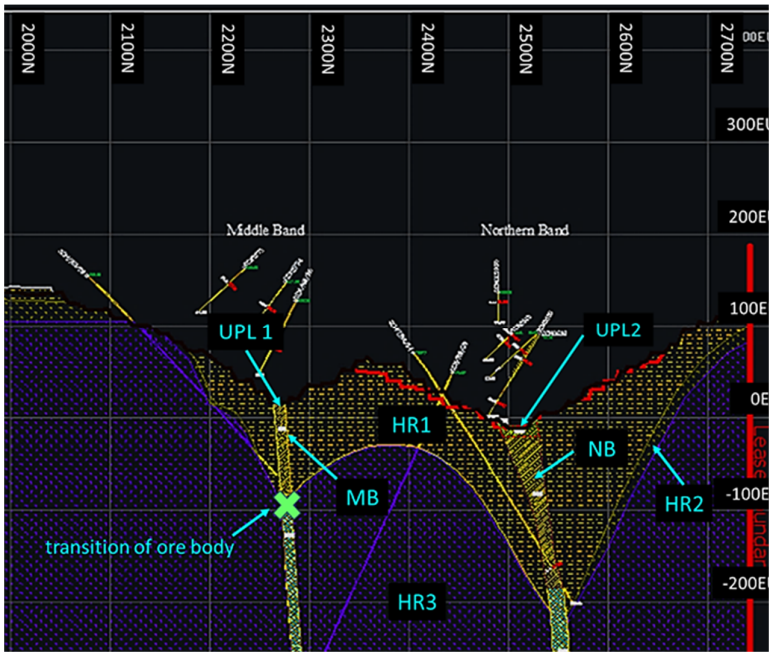

b) Vertical section of the mine prepared in AutoCAD (HR1– limonite, HR2– weak serpentinite, HR3– hard serpentinite).

Figure 1. Plan and section of the mine under study.

The definition of friable rocks was given by the Task Committee of American Society of Civil Engineers as 'highly weathered' or 'completely weathered' rock [20]; and over the years, there have been recommendations for supporting excavations made in such rocks with the most recent update published by the Norwegian Geotechnical Institute [21], which makes use of Q-value (rock mass quality), and indicates permanent support based on the documented case histories. NATM described support requirement, based on Ö NORM B2203 [22-23], for friable rocks to be immediate, systematic and cautioned against progressive fallout if not installed on time with a subsequent

support implementation in a case study in Turkey with tunnel diameters of 13-19 m [24]. Similar attempts to incorporate "friable" characteristic of rocks were made by more authors [25-28]. Construction of tunnels, mine excavations and caverns in weathered and friable rock mass with squeezing ground were documented in several countries [23, 29-31]. In 2014, Marinos [32] published detailed principles and guidelines for selecting immediate support measures, which are proposed based on the principal tunnel behaviour mode. This has been possible due to the experiences obtained from tunnels located in various flysch rock-mass types, which also experienced squeezing at greater depths. In 2000, Dalgic [22] applied the GSI system proposed by Hoek [33], after examining the weak rocks in the Beykoz Tunnel, and classified them as blocky/disturbed (GSI– 30 to 40), disintegrated (GSI– 20 to 30) and foliated/laminated/sheared rock (GSI– 10 to 20) using the GSI. The study reported that a tunnel length of 625 m having a finished span of 10.6 m was possible by providing adequate support and using appropriate excavation techniques. In Taiwan, expressway tunnels of cross-sectional area 100-160 m^2 passed through loosely cemented sedimentary rocks of strength less than 5 MPa [34]. The construction/excavation techniques were changed, so as to reduce vibrations from blasting such as using road header for cutting and even adopting double-side gallery method in poor quality rock masses. Apart from primary supports (wire-mesh, shotcrete, steel ribs, forepoling, etc.), rock tendons or self-drilling rock bolts were installed instead of the conventional grouted rock bolts. These studies demonstrate that, with the implementation of suitable measures, it is feasible to support excavations in weak and weathered rock masses.

The literature demonstrates that stope designs in rock is generally conducted, where either ore or host rock is strong and competent. The Nicholas and Hartman methods ([6] and [7]) suggested for the practical implementation of a mining method based on the rock types, geometry of the stopes, and stress conditions. However, their methods are not applicable in the present case since both host rock and ore body are friable and weak. Hence, the novelty of the proposed work is to design an underground mining method for winning ore from underground by blasting vertical long-holes in stages from the bottom of the stope towards the surface. This method, unlike the conventional transitions from surface to underground, will not leave a crown pillar at the ultimate pit level. The method also ensures that no caving in the open-pit benches occurs during underground operations. To achieve this, controlled blast designs, systematic underground working plan with paste filling, and a slope stabilisation scheme are extensively studied as part of the larger project.

The novelty of the work highlighted in this paper is to design the sequence of safe operations after analysing the stability of the underground stopes considering excavated zone, in-situ and paste-filled pillars. A new strength-based "Mining Sequence Factor (MSF)" is proposed, with a numerical range between 0 and 1, where 0 represents open stopes, and 1 signifies unmined in-situ pillars. In a series of transverse stopes, width of 20 m is considered with combinations of height of 30 m, 40 m, and 50 m. Finite Element Method (FEM) based numerical analysis of 36 models is carried out, using elasto-plastic material model and the results are analysed in terms of equivalent plastic strain that is developed on in-situ and backfilled pillars. The various mining and backfilling operations are quantified in terms of MSF, which is suggestive of the cumulative strength of the operating zone along the strike of the ore body. A relationship between MSF and the average value of equivalent plastic strain (AEPS) is obtained for various conditions. Based on the values of MSF and AEPS, a guideline is proposed to select the mining operation. The paper mainly recommends that the minimum pillar (either in-situ or backfilled) dimensions of 40 m is to be maintained at all stages operations. Apart from this, the paper also propounds a support system for the decline and underground drives that will be constructed to access the ore body in underground. The performance of the support system is analysed with the help of stress and cumulative plastic strain profiles. Suggestions are also made to restrict the unsupported length of the drivage of the decline or drives.

2. Geology and Rock Properties

The mine lies in a chromite-rich valley situated above the Precambrian banded-iron formation and ultramafic rocks containing chromite. These ultramafic rocks, which host chromite, intruded into the iron formation before significant deformation occurred and were subsequently folded together with the older sediments. The geometry of the ore bodies, host rocks and the vertical extent are previously shown in Figure 1. The strike of the ore bodies is directed towards east-west directions, while the surface benches are

made in north-south directions. The average thickness of the ore bodies MB and NB are approximately 16 m and 27 m, respectively having a dip angle of about 85°. The width of NB reduces with depth till -100 m RL but becomes constant to about 20 m thereafter. Their respective ultimate pit levels, UPL1 and UPL2, are designed to lie between 18 m RL to 35 m RL, and 25 m RL to -10 m RL along the strike. Figures 2a and b show field pictures of weathered/disintegrated and slightly consolidated nature of rock mass that exist in the overburden.

a) Highly weathered limonitic rock mass **b) Slightly consolidated limonitic rock**

Figure 2. Field pictures of overburden.

The friable nature of the ore body continues up to a depth of almost 100 m RL as marked in Figure1 by the 'transition of ore body'. Thereafter, the ore bodies become weathered and fractured, followed by hard formation beyond -150 m RL. As mentioned before, the Foot Wall (FW) and Hanging Wall (HW) rocks of MB and NB ore bodies are composed of highly weathered limonite (HR1) and serpentenite (HR2) rock mass, which is further underlain by a much more competent hard serpentinite (HR3) rock mass.

Laboratory experiments were performed to obtain the properties of various materials (ores– O1, O2, O3; host rocks– HR2, HR2, HR3; Cemented-Paste Backfill– CPB) using uniaxial compression, direct shear and triaxial tests depending on the competency and friable nature of the rocks. O1, O2, and O3 are the divisions in the ore bodies by virtue of the depth as is in the case of the host rocks. O1 is the friable region, while O3 is the hard one, and O2 holds the transition of the ore body from O1 to O3. Figure 3a shows the stress-strain relationships of O1, O2, and O3 under uniaxial compression tests. The elastic modulus and Poisson's ratio are estimated from these data and used in the numerical modelling after adjusting for rock mass conditions. In this case, GSI of O1, O2, and O3 are taken to be 25, 35, and 70, respectively. Hoek-Brown [35] m_i parameter and disturbance factor, D is considered as 20 and 0.1, respectively. Similarly, rocks of HR2 and HR3 are tested in the laboratory, as shown in Figure 3b. Table 1 lists various properties estimated from these plots. Rock mass properties of host rocks are determined as ore body. However, GSI for HR2 and HR3 rock mass are assumed to be 40 and 70, respectively, for m_i of 12 and D of 0.1.

It may be noted that for HR1, uniaxial compression test is not possible due to the extremely friable nature of the rock. Therefore, direct shear tests are conducted and results are plotted in Figure 4a. The values of cohesion (41 kPa) and angle of internal friction (24°) so obtained are used to assume the UCS and E values of the rock mass. Direct shear test results are also plotted for friable ore (O1) in Figure 4b for determination of cohesion and friction angle.

In this study, it is proposed that limonitic soil can be used as paste-backfilling material for filling the excavated stopes. In order to attain a strength of at least equal to the host rock, while ensuring the flowability of the paste, an appropriate amount of cement and water are to be mixed with the soil. For this purpose, cemented-paste backfill (CPB) materials are prepared in the laboratory with limonitic soil, cement and water respectively mixed in the ratio of 8.1:1:4.2 by weight. For the CPB material, uniaxial compression and triaxial tests are conducted after 28 days of curing. The results are plotted in Figure 5a and Figure 5b, respectively. The uniaxial compressive strength (UCS) is found to be 650 kPa, cohesion 260 kPa and angle of internal friction 12°. The final properties of all the materials used in the study are presented in Table 1 in section 3.3.

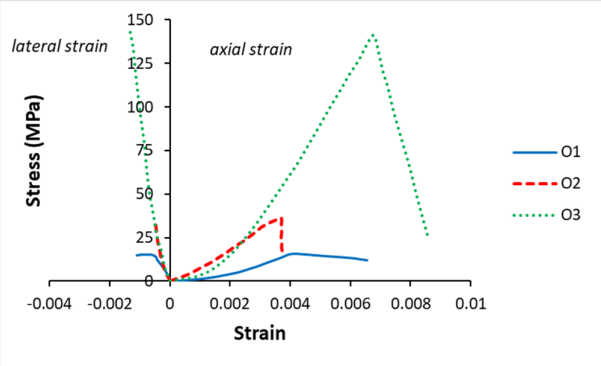

a) Uniaxial compression test results of ore (O1, O2, O3)

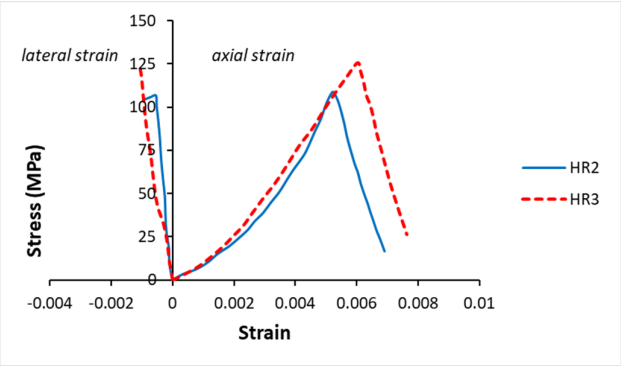

b) Uniaxial compression test results of host rocks (HR2, HR3)

Figure 3. Uniaxial compression test results of ore and host rocks.

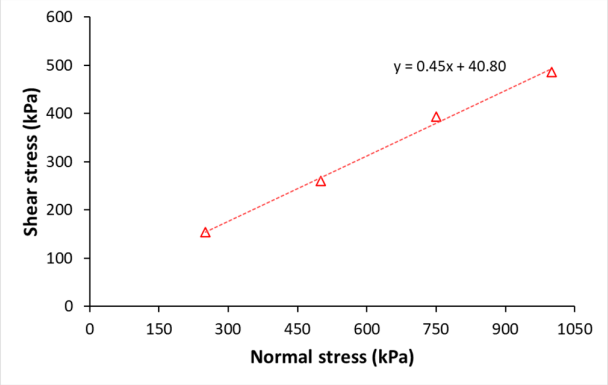

a) Direct shear test results of friable chromite ore (O1)

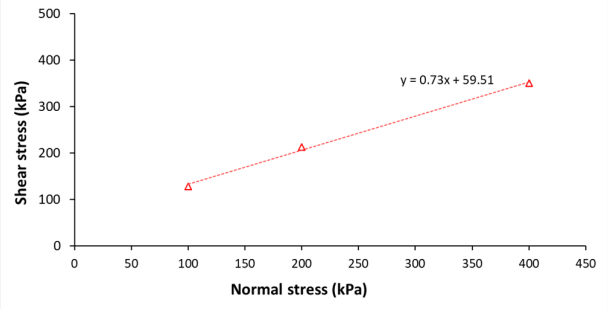

b) Direct shear test results of limonitic host rock (HR1)

Figure 4. Direct shear test results of ore and host rock.

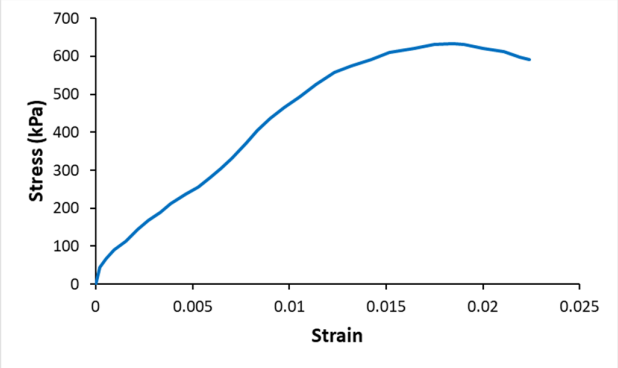

a) Uniaxial compression test result of CPB

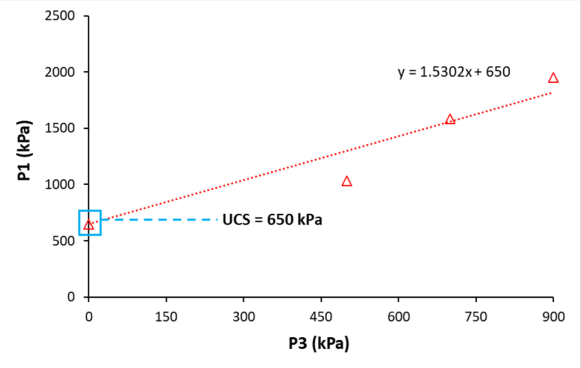

b) Triaxial test results of CPB

Figure 5. Uniaxial compression and triaxial test results of CPB after 28 days of curing.

3. Mine Design using 3D Numerical Models

The total strike length of ore bodies in the case study mine exceeds 2000 m. In this study, 400 m of the strike length, located in the middle of the pit, is considered, as the pit limit has already been reached for both ore bodies. Three-dimensional mine model is developed using seven vertical sections of the mine geometry taken at every 100 m interval along the strike between latitudes 2000N and 2700N. One such section is shown in Figure 1b. ANSYS Workbench platform is used to prepare 3D geometry of each rock layers like O1, HR1, etc. from these sections. The geometrical model depicting all rock layers is shown in Figure 6a. It is, upon detailed discussions, decided that the underground mine for the friable ore bodies will be accessed using a decline. The location, dimensions, and support requirements of the decline are the potent decisions to be taken in this study. Apart from that, the stope and pillar dimensions, and

sequence of mining for safe operations are the other important but most critical decisions. In the following, the dimensions of stopes, pillars, and support requirements of the decline, drives, and cross-cuts are decided based on the 3D numerical modelling techniques and detailed discussions therewith.

3.1. Decision on stope design

It is decided that a decline will be constructed in between the MB and NB ore bodies for transporting men, materials, and ores. Figure 6b depicts the decline, crosscuts, and drives for servicing the MB ore body. The pit bottom of the MB ore body is 15 m RL, and hence, a cross-cut is made at -35 m RL (giving a stope height 50 m) from the decline to reach the footwall drive. From the footwall drive, extraction cross-cuts will be made at every 20 m centre-to-centre at an angle of about 60º along the strike to access the ore body as shown in Figure7, and thereby generating individual stopes. The stope width is decided to be kept 20 m along the strike. The stopes are named as "Primary": P1, P2, P3, and so on, 'Secondary": S1, S2, S3, and so on, and "Tertiary": T1, T2, T3, and so on. They are marked in Figure 7 for the NB as well as MB ore bodies. The details of the numerical analysis leading to this decision are discussed in the succeeding section along with the definition of primary, secondary, and tertiary stopes. How far the next stope should be mined i.e. the pillar width is decided after analysing a series of mining and backfilling sequences. This pillar width is varied between 30 m, 40 m, and 50 m, which gives rise to three major sequences. The main idea is to extract the primary stopes first, while maintaining sufficient pillar in between two consecutive primary stopes. After the filling of primary stopes, secondary stopes will be mined in sequence, and so on. The success of the proposed mining method depends heavily on the stability of the pillar (in-situ and backfilled), eventually giving rise to the final mining sequence. Two ventilation shafts are also proposed in the two corners of the two ore bodies.

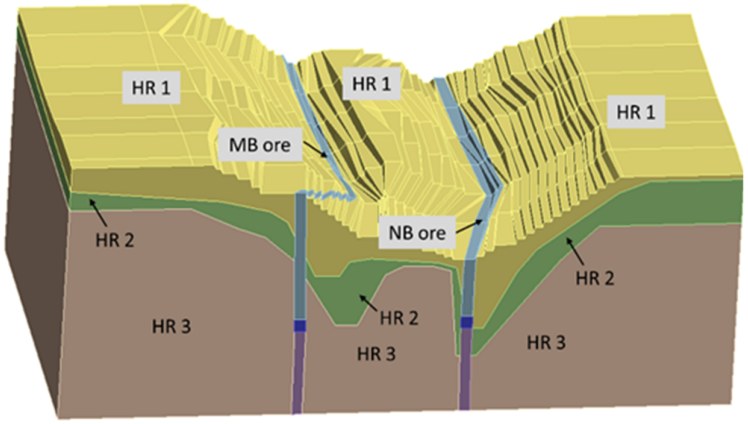

a) 3D mine model showing surface mine slopes.

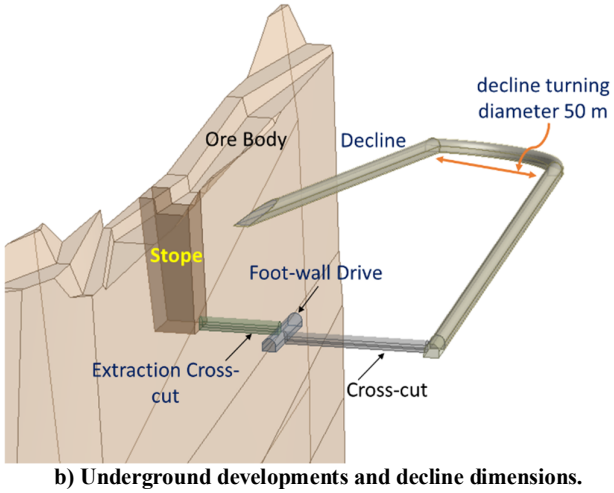

b) Underground developments and decline dimensions.

Figure 6. 3D mine model showing existing surface mine and the proposed underground developments.

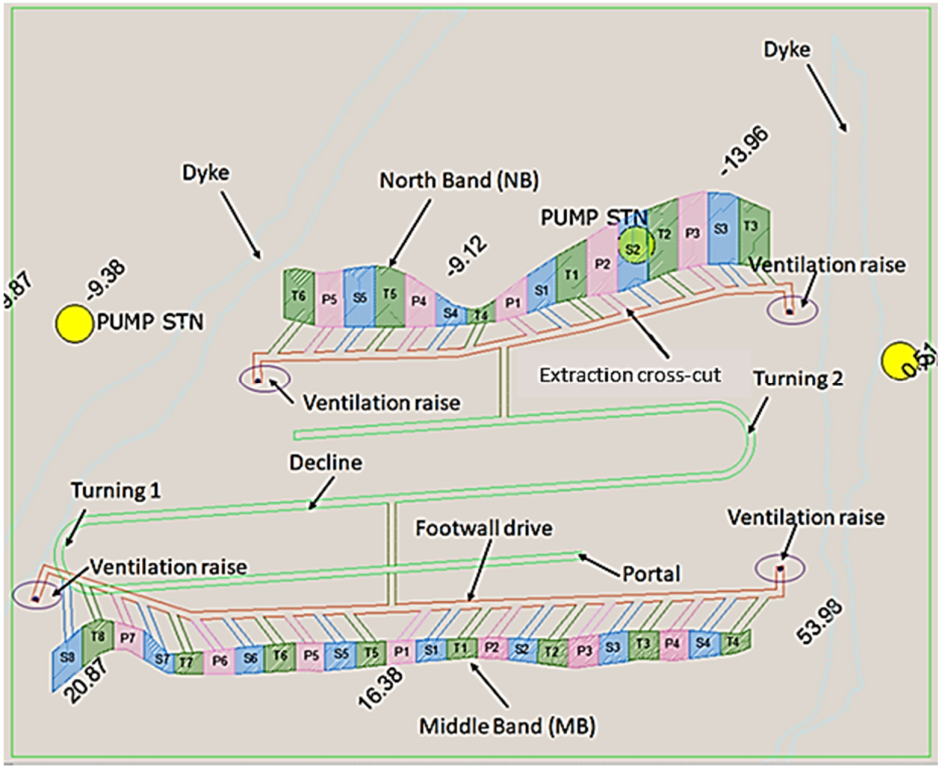

Figure 7. Stopping sequence for MB and NB.

3.2. Sequence of mining and backfilling

As mentioned before, the width of each stope along the strike of the ore body is decided to be 20 m. The decision of stope width of 20 m is taken considering the restriction due to regulatory guidelines and desired production needs. It is also decided that, for a better ground control, one stope will be mined at a given time. Hence, the sequence of mining and filling of stopes must be chosen judiciously to maintain a level of safety in and around the Stopping zone. In this study, three broad sequences are assumed, namely:

Q1 (consecutive sequence): distance between two primary stopes is 20 m.

Q2 (alternative sequence): distance between two primary stopes is 40 m.

Q3 (subsequent sequence): distance between two primary stopes is 60 m.

The mining and filling operations for each sequence are illustrated in Figure 8. A stope is termed as "primary (P)" stope if both sides along the strike have unmined stopes. A "secondary (S)" stope is defined if one side has unmined stope, and the other side has a filled stope. A stope is called "tertiary (T)" if both the sides have filled stopes. For analysis purposes and comparison of various sequences, it is decided to perform (mining and backfilling) operations on a fixed ore length of 120 m along the strike. In Figure 8, mining and filling operations are carried out along 100 m strike length along with 10 m pillars left unmined on either end. In Figure 8a., four distinct operations are shown in Q1 or consecutive sequence plan, as stated below:

Operation 1: Mining of primary (P) stopes, i.e. Q1PM.

Operation 2: Filling of primary (P) stopes with backfill material, i.e. Q1PF.

Operation 3: Mining of tertiary (T) stopes after filling of the primary stopes, i.e. Q1TM.

Operation 4: Filling of tertiary (T) stopes, i.e. Q1TF.

Operation 1 is named as Q1PM, where Q1 indicates sequence 1, and PM indicates primary (P) stopes after mining (M) leaving 20 m unmined pillar on either side. In the nomenclature Q1PF, letter F indicates filling. Operation 3 is named as Q1TM, where tertiary (T) stopes are mined (M) only after filling the primary stopes. Operation 4 is termed as Q1TF, indicating filling (F) of tertiary (T) stopes. Similarly, Figures 8b and 8c show the operations for alternative and subsequent sequences. For each of the sequences, Q1, Q2, and Q3, stope height is varied as 30 m, 40 m, and 50 m, which are designated as H1, H2, and H3, respectively. This gives rise to the final nomenclature of models. For example, Q1H1TF

implies an operation in sequence 1 having stope height of 30 m, where primary and tertiary stopes are filled. The various mining and backfilling operations of three sequences (Q1, Q2, and Q3) shown in Figure 8 are developed and analysed using the Drucker-Prager material models in ANSYS. Altogether, 36 numerical models are selected for comparison purposes. The details of models are provided in section 3.3.

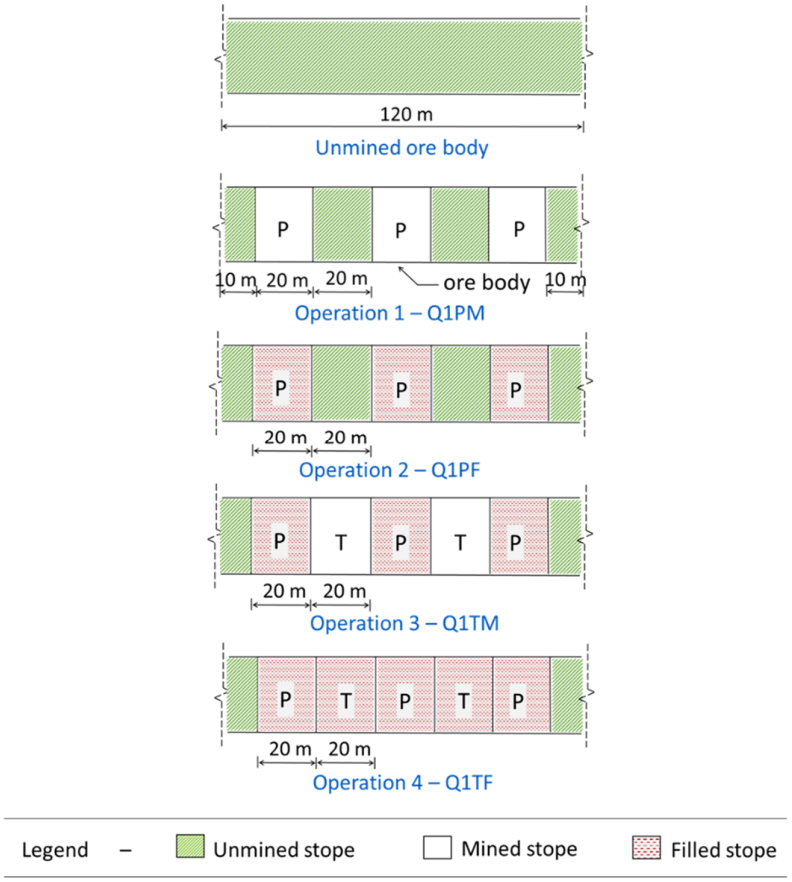

a) Sequence 1 (Q1).

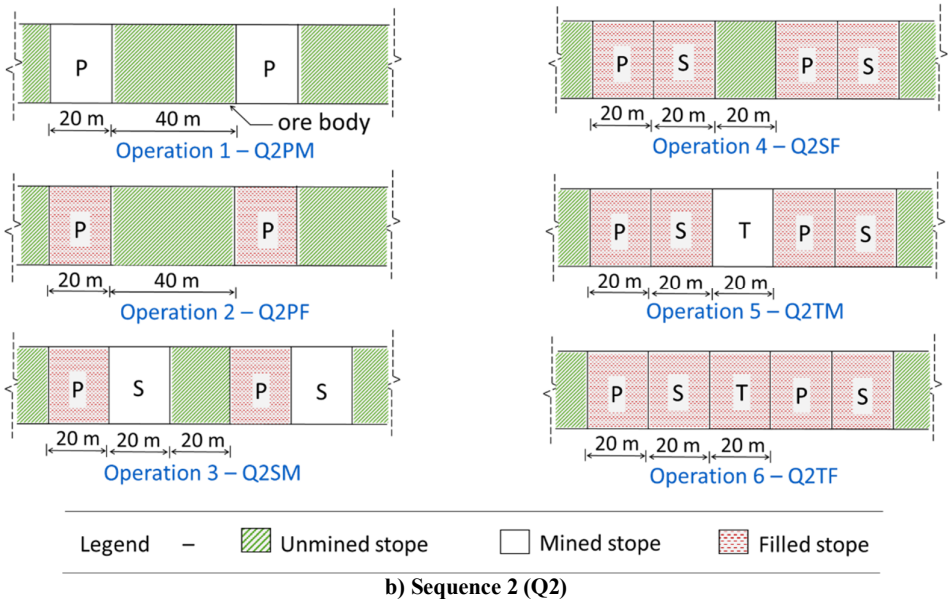

b) Sequence 2 (Q2)

Figure 8. The operations of the three Stopping sequences.

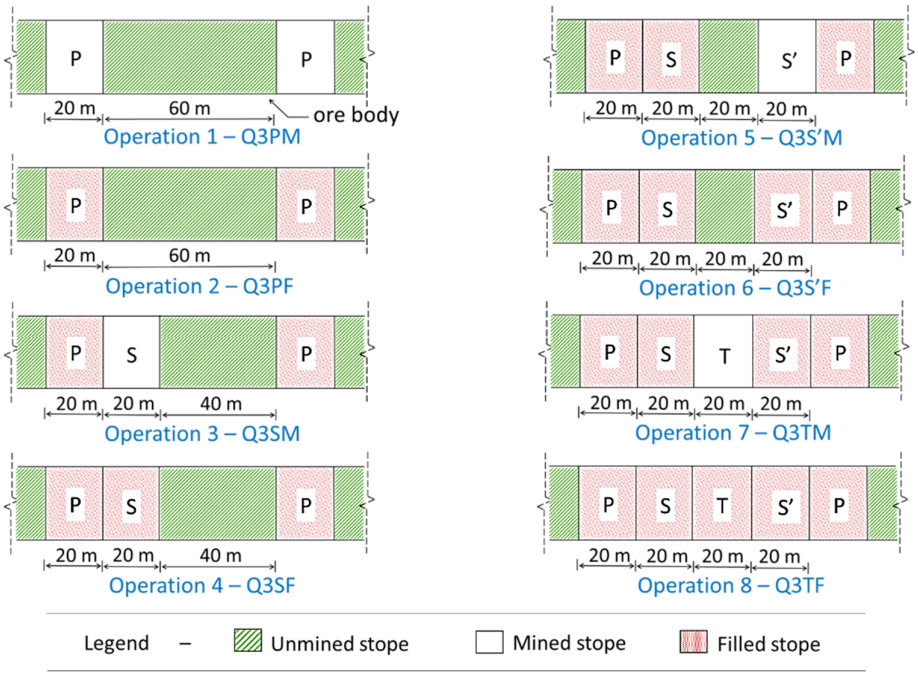

c) Sequence 3 (Q3).

Continues of Figure 8. The operations of the three Stopping sequences.

3.3. Material properties and elasto-plastic model

An example of a 3D numerical model for simulating operations on MB ore body, having components same as the mine model in Figure 6a, is developed and shown in Figure 9a. An elasto-plastic analysis is carried out using the Drucker-Prager yield criterion [36]. Table 1 gives the material properties used in the analysis, the details of which are included in section 2.

The boundary conditions for the model are given in Figures 9b and 9c. In the model, horizontal stresses are applied on vertical sides, and the corresponding opposite sides are fixed in the normal direction as shown in Figures 9b and 9c. However, horizontal stresses are applied below the ultimate pit level since, due to surface mining, the continuity of rock strata is disturbed. Figures10a, 10b, and 10c show the ore body MB in 3D numerical model (Figure 9a) prepared for sequence 1 (Q1) operations Q1H1PM, Q1H1TM, and Q1H1TF, where stope height is 30 m (H1).

Table 1. Material properties used in 3D modelling.

Material	Density (kg/m^3)	Young's modulus (E) (MPa)	Poisson's ratio	UCS (MPa)	Cohesion (c) (kPa)	Friction angle ϕ (°)
O1	3000	700	0.30	1.40	41	24
O2	3000	1500	0.10	6.60	890	40
O3	3600	13398	0.20	50.00	3516	58
HR1	2000	250	0.35	0.73	60	36
HR2	2000	1500	0.12	3.00	780	35
HR3	2900	25400	0.15	43.00	3800	55
CPB	1500	50	0.25	0.65	260	12

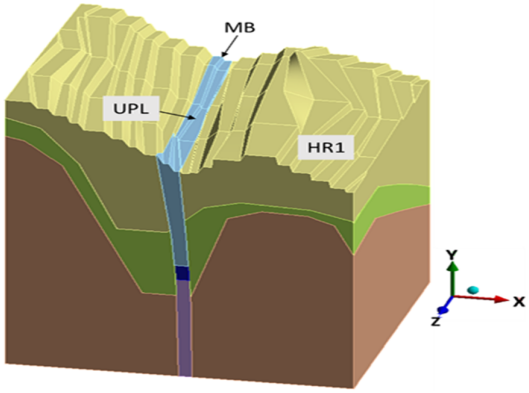

a) 3D model to analyse mining and filling operations

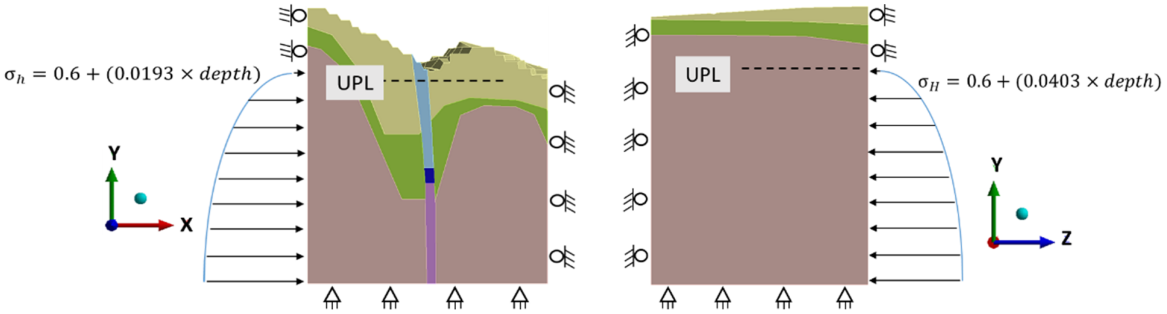

b) Boundary conditions along Z axis

c) Boundary conditions along X axis

Figure 9. Models analysed for mining and filling operations.

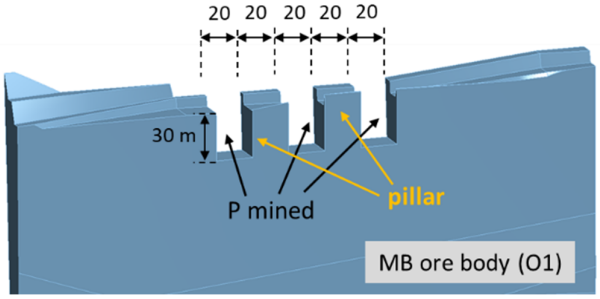

a) Primary stopes mined (Q1H1PM)

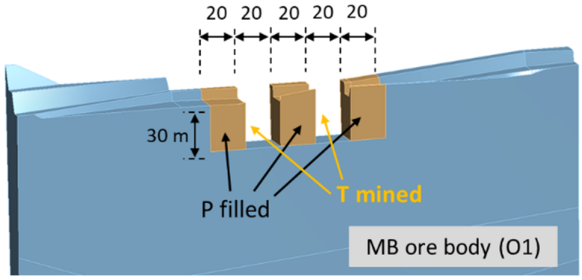

b) Primary stopes filled and tertiary stopes mined (Q1H1TM)

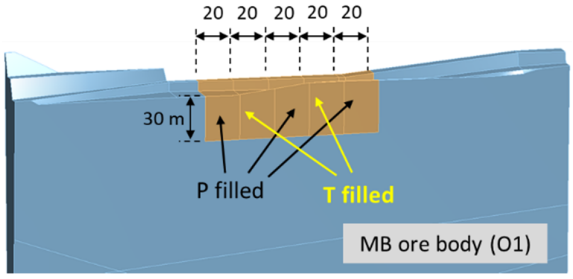

c) Primary and tertiary stopes filled (Q1H1TF)

Figure 10. Operations of sequence 1 (Q1) on stope height 30 m (H1) performed on MB ore body

3.4. Material model

In this study, the Drucker-Prager yield criterion [36], as given in Equation 3.4.1, is used for evaluating the onset of rock failure.

$$\sqrt{\frac{J_2}{3}}\left(2 + N_\phi\right) - \sigma_m\left(N_\phi + 1\right) - 2c\sqrt{N_\phi} = 0 \qquad (3.4.1)$$

where, σ_m , N_ϕ, and J_2 are, respectively, the mean normal stress, triaxial factor, and second invariant of stresses, as given below:

$$\sigma_m = \frac{\sigma_1 + \sigma_2 + \sigma_3}{3} \quad (3.4.2)$$

$$N_\phi = \frac{1 + \sin\phi}{1 - \sin\phi} \quad (3.4.3)$$

$$J_2 = \frac{1}{6}[(\sigma_1 - \sigma_2)^2 + (\sigma_2 - \sigma_3)^2 + (\sigma_3 - \sigma_1)^2] \quad (3.4.4)$$

where, $\sigma_{1,2,3}$ are principal stresses, ϕ is the angle of friction.

The above DP criterion has been implemented in ANSYS Workbench platform, where uniaxial compressive strength, biaxial strength, and tensile strength are the necessary inputs. In the absence of laboratory-experimented biaxial strength data, Equation 3.4.11 [37] is used to estimate the biaxial strength (f_{bc}). Tensile strength (T) of limonite and chromite ores is assumed to be negligible. However, in this study, to implement the DP criterion, it is considered to be one tenth of the uniaxial compressive strength, UCS as is done for other rocks, which still comes out to be negligible.

$$f_{bc} = \frac{3 \times UCS}{4 - N_\phi} \quad (3.4.11)$$

The elasto-plastic material properties are thus estimated. Elasto-plastic material behaviour is assigned to HR1, HR2, O1, and O2, while the rest are kept elastic since stress level is too low as compared to their uniaxial compressive and tensile strength.

3.5. Quantification of mining and filling sequence: mining sequence factor

As is evident from Figure 8, given any operation, a 20 m-wide operated condition (mined/unmined/filled) will be surrounded by one of the three conditions, namely, in-situ pillar (or unmined stope), filled stope (or backfilled pillar), and mined/empty stope. For instance, an in-situ pillar may exhibit five different conditions, as illustrated in Figure 11a, and a filled stope may have six conditions, as shown in Figure 11b. The strength of each pillar/stope condition as well as the strength contributed by the surrounding conditions along the strike (left and right) must be accounted for. This influence by virtue of strength is taken care of by a new metric called the Mining Sequence Factor (MSF), which overall helps differentiate between the various 36 operations. Only the conditions along the strike within the ore body are considered, as the host rock conditions remain unchanged for all operations. The MSF is calculated as follows.

i) Calculation of fill factor, η

The three operated conditions unmined, mined and filled are assigned a "fill factor". Considering a mined-out open stope has no strength, it is defined as:

$$\eta = \frac{strength\ of\ operated\ condition}{strength\ of\ unmined\ condition} \quad (3.5.1)$$

The strength is derived from the UCS of the material forming the operated condition, i.e. strength of unmined condition is UCS of O1 (1400 kPa), of filled condition is UCS of CPB (28-day strength is 650 kPa), and that of mined condition is zero due to absence of any material Hence, η = 0 for mined-out stope, η = 0.464 for filled stope (or backfilled pillar) and η = 1 for unmined stope.

ii) Calculation of nominal strength factor, σ

Now, consider Figures11a and 11b, where different conditions that may arise around an in-situ pillar and a filled stope are depicted. The strength imparted by these conditions on to an operated condition is taken care of by a nominal strength factor, σ, and is estimated using:

$$\sigma = \frac{\sum(l_i \times \eta_i)}{\sum l_i} \quad (3.5.2)$$

where, l_i = width of the unmined pillar or backfilled stope i, and width of mined/filled/unmined stope, η_i = fill factor for the corresponding pillar/stope. For example, in condition number 5 in Figure 11b, for the filled stope itself in the middle, l_i = 20 m, but the effect of the condition on either side is taken into account only for one-half of the whole width of the condition and l_i = 10 m here, giving $\sum l_i$ = 40 m. Thus σ = 0.482 for condition number 5. Following suit, σ is calculated for each of the five 20 m-wide stopes/pillars and 10 m-wide unmined pillars on the ends along the 120 m length fixed for comparison of different mining/backfilling sequences as shown in Figure 8.

iii) Calculation of mining sequence factor

Finally, MSF is calculated as a weighted average of σ along the entire length of 120 m for which the models are analysed, and is given as:

$$\text{MSF} = \frac{\sum(m_i \times \sigma_i)}{\sum m_i} \qquad (3.5.3)$$

where, $\sum m_i$ = 120 m.

For example, in Figure 8a, operation 5–Q1TM, the value of MSF is calculated as:

$$\text{MSF} = \frac{(10 \times 0.87) + (20 \times 0.482) + (20 \times 0) + (20 \times 0.232) + (20 \times 0) + (20 \times 0.482) + (10 \times 0.87)}{120}$$

$$\text{MSF} = 0.344$$

Here, an MSF of 1 indicates no mining has taken place, i.e. in-situ condition, and that of 0 indicates no pillar is left behind, which, in reality, is not practical. MSF, in a way, is an indicator of how much strength is retained in situ by backfilling, as compared to the in-situ condition for each operation of mining or backfilling. The MSF is also independent from stope height.

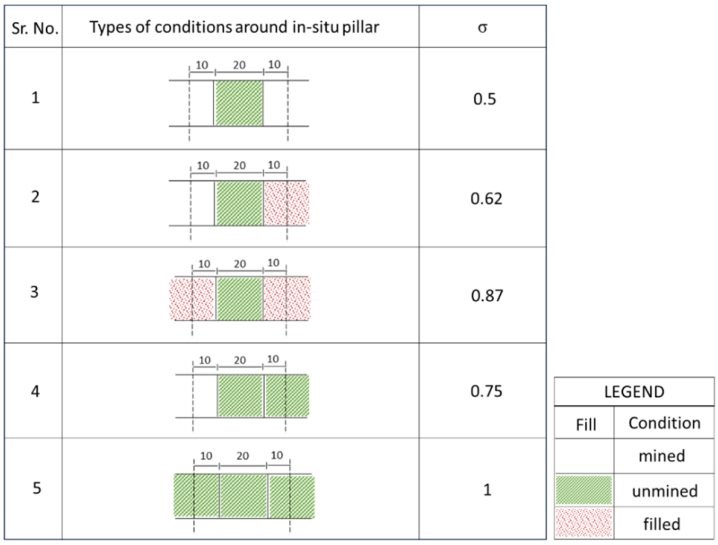

a) Around an in-situ pillar.

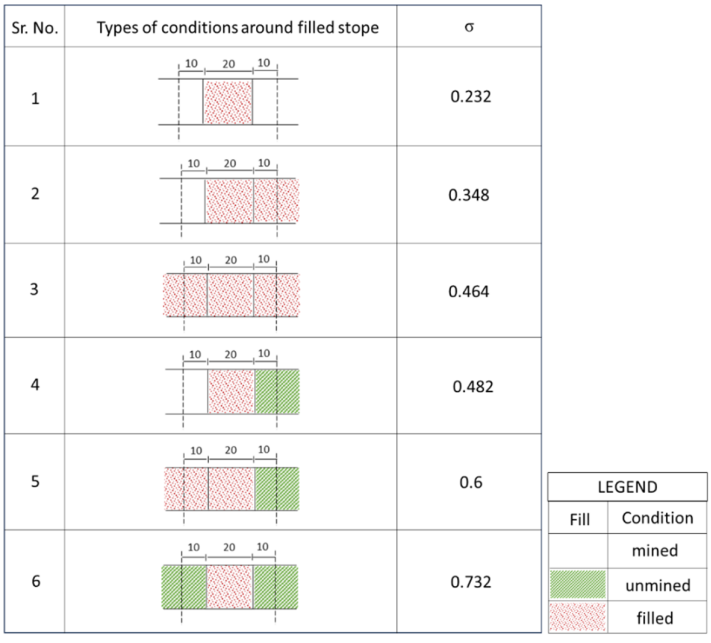

b) Around a filled stope.

Figure 11. Values of nominal strength factor σ for different conditions.

The least MSF value is found to be 0.29 in models Q1PM for all the stope heights H1, H2, and H3, and the highest value is 0.577 in models Q1TF, Q2TF, and Q3TF for all the heights. Different values of MSF are calculated for all the models or operations of all the three sequences Q1, Q2 and Q3.

3.6. Estimation of average EPS of the stope and pillar systems

From each of the 36 numerical models, Equivalent Plastic Strain (EPS) profiles are extracted 1 m below the surface level at the middle of the MB ore body. Typical profiles for Q1H3TM, and Q2H3PM are shown in Figure12. It is clear that at the corners of the in-situ pillars and filled stopes, plastic strain accumulates creating a favourable condition for pillar spalling. The average value of EPS is estimated over 120 m length of the mining sequence and they are found to be 1.0×10^{-3} and 5.8×10^{-4} for Q1H3PM and Q2H3SM models, respectively. Similarly, average EPS (termed as AEPS) are estimated for all 36 models and plotted with MSF, as shown in Figure13.

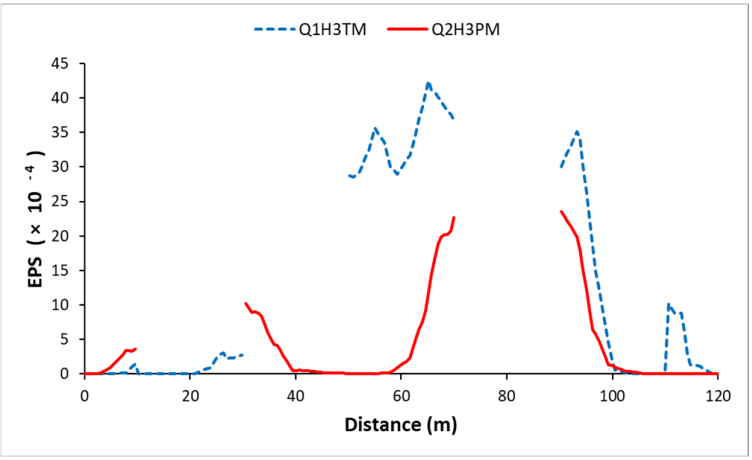

Figure 12. Distribution of EPS

Table 2 lists the maximum and minimum AEPS values with height of stope and MSF. Figure13 shows the variation of MSF with AEPS for all the three stope heights H1, H2 and H3. The figure clearly shows that the magnitude of the slope of AEPS and the corresponding intercept increases with the height of the stope. The slope changes negatively 1.7 times if stope height changes from 30 m to 50 m.

Table 2. Maximum and minimum AEPS for each stope height and corresponding MSF.

Stope height	AEPS ($\times 10^{-4}$)		Model	MSF
H1	max	7.90	Q1H1PM	0.290
	min	0.32	Q1H1TF, Q2H1TF, Q3H1TF	0.423
H2	max	9.30	Q1H2TM	0.344
	min	0.48	Q1H2TF, Q2H2TF, Q3H2TF	0.423
H3	max	12.00	Q1H3TM	0.344
	min	0.31	Q1H3TF, Q2H3TF, Q3H3TF	0.423

The plot of AEPS vs MSF is an attempt to provide a tool for selecting a particular sequence of mining that can be chosen to safely mine the ore body by 20 m wide transverse Stopping method. In order to distinguish the favourable zones, in which AEPS is allowable for mining, the distribution of EPS in the 3D numerical models are shown in Figures14a, 14b, and 14c. From Figure14a (model Q1H2TM), it is clear that an AEPS of 9.3×10^{-4} occurs for an MSF of 0.344. The concentration of EPS is found to be developed in the order of 0.002 to 0.006 at the corners of the pillars, and also extending to the end pillar. On the other hand, the models Q2H3PM and Q2H3TM are not so severe (Figure14b and 14c). It is found to be in the order of 0.001 to 0.004 in the corner of the pillars. The AEPS is 3.6×10^{-4} and 5.0×10^{-4}, respectively in these two models for MSF of 0.52 and 0.461. Overall, an AEPS of 4×10^{-4} and below develops if the pillar (in situ or backfilled) width is 40 m or above. In contrast, uniaxial tests of chromite rock suggest a total strain of 0.38% at failure. In the

same token, triaxial test results of backfill sample gives a total strain of 1.84% at failure. Therefore, considering unforeseen circumstances on field and blasting aspects, threshold AEPS value is decided to be 8×10^{-4}, which is five times safer than 0.38% strain from uniaxial test results of chromite. As a result, it is decided that any operation with MSF below 0.35 and AEPS above 8×10^{-4} would not be safe. Hence, the zone belonging to this definition is termed as "severe", and is not recommended. On the other hand, an AEPS below 4×10^{-4} would mean absolutely safe operation and termed as "ideal" operational zone (Figure13). However, an AEPS in between 4×10^{-4} and 8×10^{-4} can also be considered for mining operation, since there is at least a 40 m pillar in between two open stopes. This zone is termed as "moderate" operational zone. In Figure13, the shaded zone represents the mineable zone for the friable ore bodies using transverse Stopping method.

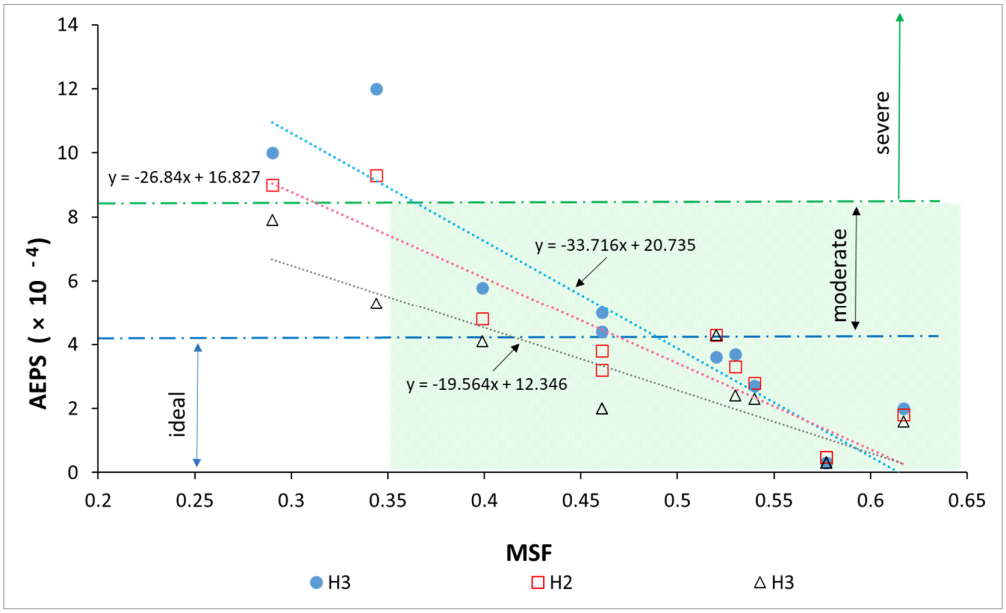

Figure 13. Variation of EPS with respect to MSF indicated for the different operations.

Based on the above observations, it is compelling to maintain the pillar width (either in-situ or backfilled) of 40 m or more at all times to stay in the safe zone, depicted by the shaded zone in Figure13. Along these lines, sequence Q2, also while considering the desired production level, is then recommended as the mining and filling operations for safely extracting the ore bodies, MB and NB. Sequence Q3 can also be adopted, however, initial development work would be much higher as compared to sequence Q2.

4. Sensitivity Analysis

A sensitivity analysis based on the properties of backfill material (CPB) and friable ore (O1) is conducted to determine changes in EPS on the pillars. Three different sets of properties are taken into consideration for the sensitivity analysis viz. i) M-10 signifies the properties, mainly modulus of elasticity and UCS, are reduced by 10% from M0, ii) M0 implies the material properties mentioned in Table 1, and iii) M+10 includes the models where properties are increased by 10% from M0. Table 3 lists the properties used for this analysis.

Table 3. Properties used for sensitivity analysis

Model set	Materials	Young's modulus (MPa)	UCS (MPa)
M-10	O1	630	1.26
	CPB	45	0.58
M0	O1	700	1.40
	CPB	50	0.65
M+10	O1	770	1.54
	CPB	55	0.72

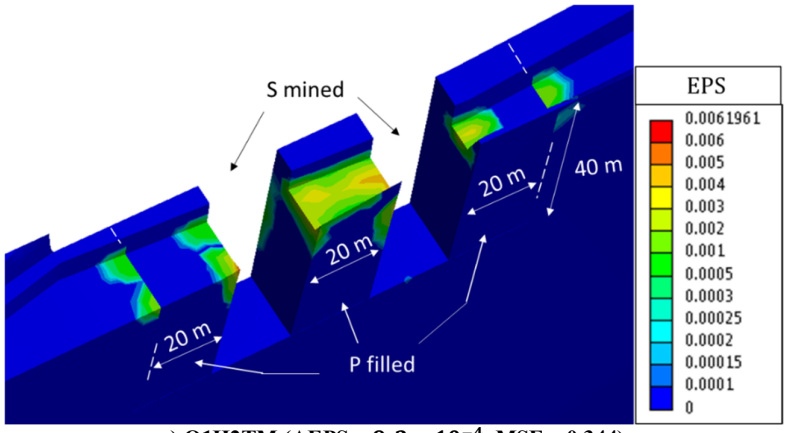

a) Q1H2TM (AEPS = 9.3×10^{-4}, MSF = 0.344).

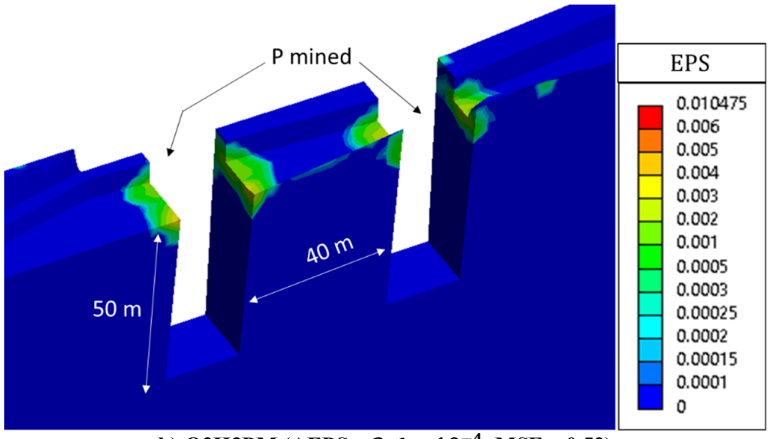

b) Q2H3PM (AEPS = 3.6×10^{-4}, MSF = 0.52)

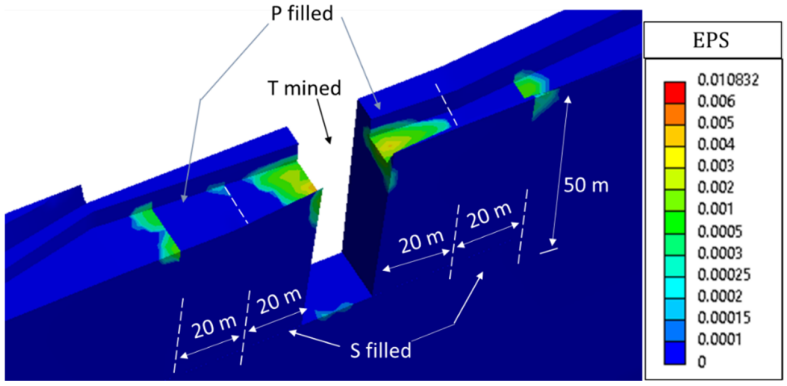

c) Q2H3TM (AEPS = 5.0×10^{-4}, MSF = 0.461).

Figure 14. Distribution of equivalent plastic strain in numerical models.

EPS results are presented for the recommended sequence (Q2) for the maximum stope height (H3). The mine sequence model, Q2H3TM possesses the maximum AEPS among all the mining operations for Q2, while Q2H3PM possesses the least AEPS apart from the fully backfilled condition. EPS results are plotted for Q2H3PM and Q2H3TM in Figures15a and 15b, respectively. As before, the maximum EPS is observed at the corner of pillars for the operations, and the M-10 model shows the highest among the three cases analyzed. The corresponding AEPS is also calculated and compared for M-10, M0, and M +10 in Table 4.

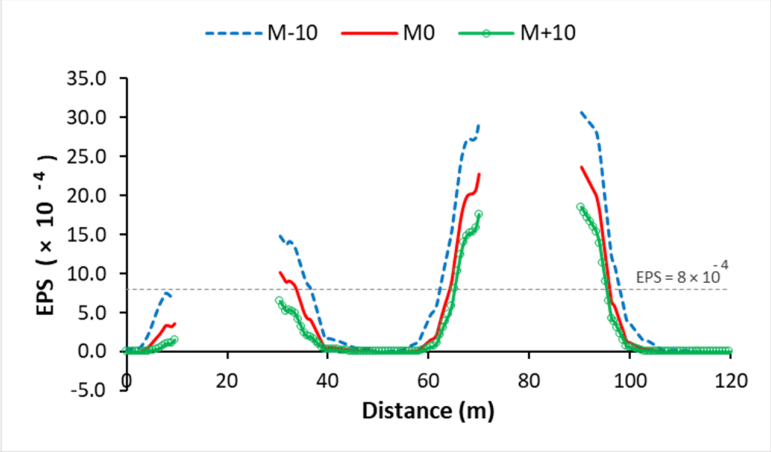

a) Distribution of EPS for Q2H3PM

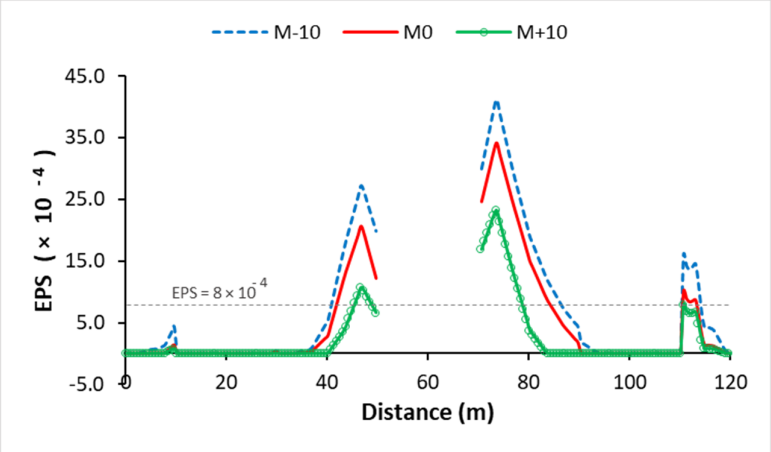

b) Distribution of EPS for Q2H3TM

Figure 15. EPS results for M-10, M0 and M+10

Table 4. Maximum EPS and AEPS observed on varying properties.

Model set	Parameter	Q2H3PM	Q2H3TM
M-10	Maximum EPS	23×10^{-4}, 30% increase	40×10^{-4}, 25% increase
	AEPS	6.5×10^{-4}, 60% increase	6.9×10^{-4}, 38% increase
M0	Maximum EPS	23×10^{-4}	32×10^{-4}
	AEPS	4.0×10^{-4}	5.0×10^{-4}
M+10	Maximum EPS	18×10^{-4}, 22% decrease	23×10^{-4}, 22% decrease
	AEPS	2.7×10^{-4}, 33% decrease	2.4×10^{-4}, 52% decrease

Apart from the observations made in Table 4, it is found that in case of operation Q2H3PM, there is sharp increase in AEPS to 6.5×10^{-4} when properties of the ore and backfill material are simultaneously reduced by 10%. However, in both cases of Q2H3PM and Q2H3TM, AEPS still lies below the critical AEPS value of 8×10^{-4}. It is found that the radius of influence of strain exceeding the critical EPS value (8×10^{-4}) increases only by 0.5 m, and reduces by 1.5 m when the properties are decreased and increased by 10%, respectively. On the other hand, in case of the most critical operation Q2H3TM, the increase is by 2 m and reduction by 6 m for M-10 and M+10, respectively. The above analysis suggests that even if material properties vary in the field, mining method suggested in this paper is applicable since AEPS will not exceed 8×10^{-4} and the radius critical yield zone will remain within 6 to 8 m of the excavated zone.

On the other hand, the result of this study is under consideration by a chromite mining company for possible field trial. The mine officials have accepted the design guidelines presented for stopes, pillars and sequence of operations. Upon receiving the permission from regulatory agency,

the company may start field operation first by developing the decline, followed by stopping operations.

5. Decision on Support Requirements of Decline, Drives, and Cross-cuts

The dimensions of decline, drive and cross-cut are decided to be 5 m x 3.5 m for a yearly production of 0.75 million tonne. According to NGI [21] chart for support design, the rock mass quality is "very poor", and it suggests the support category 7, which is a combination support system of fibre-reinforced concrete of thickness not less than 15 cm, reinforced ribs of sprayed concrete and bolting. However, in the present study, fibre-reinforced concrete will not be appropriate as well as bolts may not anchor in the rock mass. Therefore, a permanent support system comprising of RCC (Reinforced Cement Concrete) liner and steel arches is recommended for the excavation walls and plain concreting for the floor.

Apart from the permanent support, the stability of any excavation during operation also depends on the exposed or unsupported area during construction [38]. It is proposed to make a development of 1 m and support it before advancing for the next 1 m. As soon as the development of 1 m is made, it is recommended to support with RCC liners.

5.1. Support performance analysis using 3D numerical models

In order to conduct the study on support requirements, a section of underground development, specifically a decline, is modelled. The model consists of limonitic host rock, and has a depth of 100 m, with side-walls extending horizontally for 50 m on each side (Figure16a). The decline is excavated within the host rock, spanning a length of 50 m and sloping at 1 in 8. It is subjected to an overburden load of 50 m, which also represents the height of the stope. Horizontal stress across the decline is neglected due to open area towards the surface benches. Vertical gravity load is applied to the model based on the rock density. The RCC liner is simulated as a composite material comprising of RCC and concrete. Steel arches, assumed to be I-section beams with a uniform thickness of 20 cm, are placed at every 1 m along the decline's length. A representative model of the support is shown in Figure16b.

The steel arch, an I-beam, is assumed to have a uniform thickness of 20 cm. I-beams are often made from grade ASTM A992, which has a yield strength of 340-450 MPa, compressive strength of 250-400 MPa, Young's modulus of 200-210 GPa, tensile strength of 400-550 MPa. The typical density of ASTM A992 steel can be estimated to be around 7850 kg/m³, which is the standard density for many structural steels. The RCC component is assumed to behave as a structural beam. As per IS 456 [39], the percentage of reinforcement in an RCC beam ranges from around 0.5% to 4% of the cross-sectional area of the beam. For this study, 1% of reinforcement is assumed, and M40 concrete is assumed. Thereby, the density of RCC is calculated as a weighted value of steel reinforcement and concrete. Similarly, the value of Young's modulus and compressive strength of RCC are calculated to be 29 GPa and 43 MPa, respectively, and listed in Table 5. Young's modulus of concrete is given as $5000 \times \sqrt{f_{ck}}$ [39], where f_{ck} is characteristic compressive strength of concrete. This gives Young's modulus of RCC composite as 31 GPa but the conservative value of 29 GPa is chosen for this analysis. The concrete floor is assumed to be made of M25 concrete and the standard material properties of M25 concrete are used. The material properties of the steel arches, RCC, and concrete used in the analysis are presented in Table 3. The properties of HR1 are previously mentioned in Table 3 along with other rock mass materials. The analysis considers the Drucker-Prager yield criterion for the limonitic rock mass, while considering the support elements as elastic materials. The results are evaluated for four different conditions: i) the entire length of the decline is unsupported (S0), ii) the last 1 m of the decline is unsupported (S1), iii) the last 2 m from the face of the decline are unsupported within the friable limonitic rock mass (S2), iv) the entire length of the decline is supported (S3). The results are analysed using following parameters: the minimum principal stress (σ_3) and the Equivalent Plastic Strain (EPS).

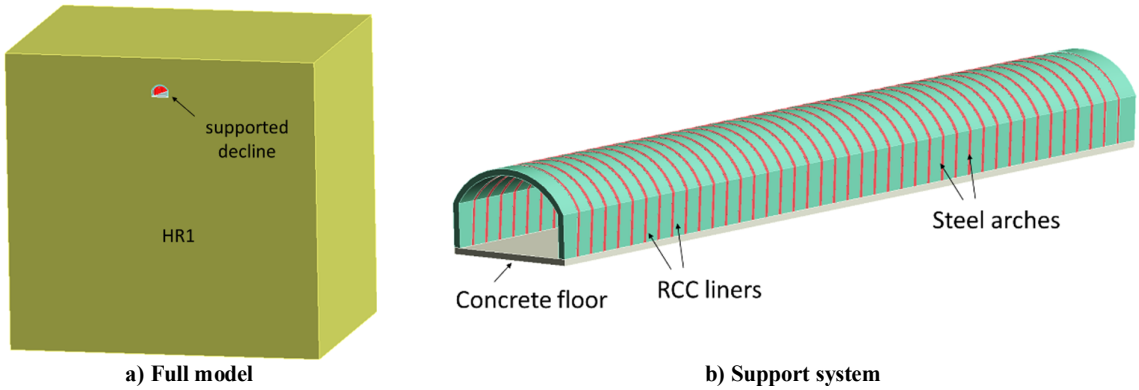

a) Full model b) Support system

Figure 16. 3D model to analyse the performance of the proposed support system.

Table 5. Material properties of support components.

Component	Density (kg/m^3)	Young's Modulus (GPa)	Compressive strength (MPa)	Tensile strength (MPa)
Steel arch	7800	200	250	400
RCC liner	2900	29	43	4
Concrete floor	2000	25	30	3

Figures17a and 17b illustrate the distribution of EPS in the rock mass surrounding the cross-section, representing the S3 and S0 models. It is evident that the combination of composite RCC and steel arches significantly reduces plastic strain along the roof and walls of the decline. The distributions of minor principal stress and cumulative effective plastic strain at 0.5 m inside the host rock along the decline axis are plotted in Figure18a and 18b, respectively. The results indicate that the development of plastic strain in an unsupported decline near the face is 0.15%, which is thirty times higher compared to the fully supported model. Similarly, the minor principal stress is also higher for the 2 m unsupported model.

Table 6 summarizes the impact of unsupported length on various result parameters for the four conditions. It is evident that leaving the decline unsupported by 1 m from the face (S1) is almost as safe as the fully supported condition (S3), while an unsupported length of 2 m (S3) results in an undesirable increase in stress and strain values. Therefore, the fundamental principle guiding the installation of the support system is to ensure that no more than 1 m of face remains unsupported at any given time. Additionally, RCC liners provide an approximate factor of safety of about 4-5, whereas steel arches offer a factor of safety well above 100. Consequently, the support system is deemed safe for all underground developments.

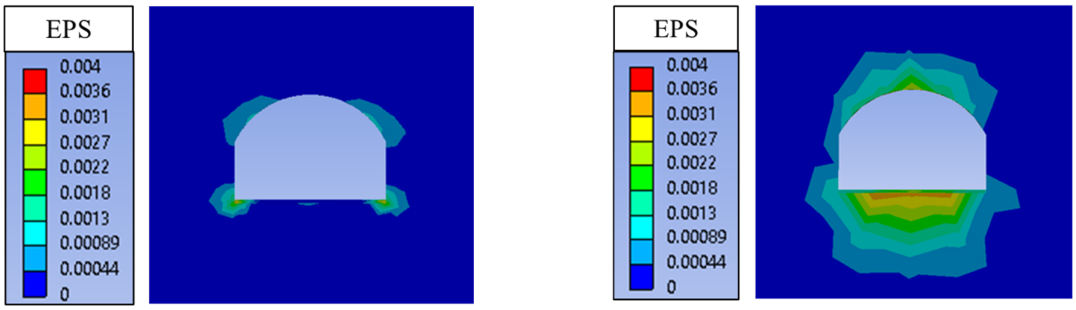

a) Across decline in condition S0 b) Across decline in condition S3

Figure 17. Distribution of equivalent plastic strain in limonitic rock.

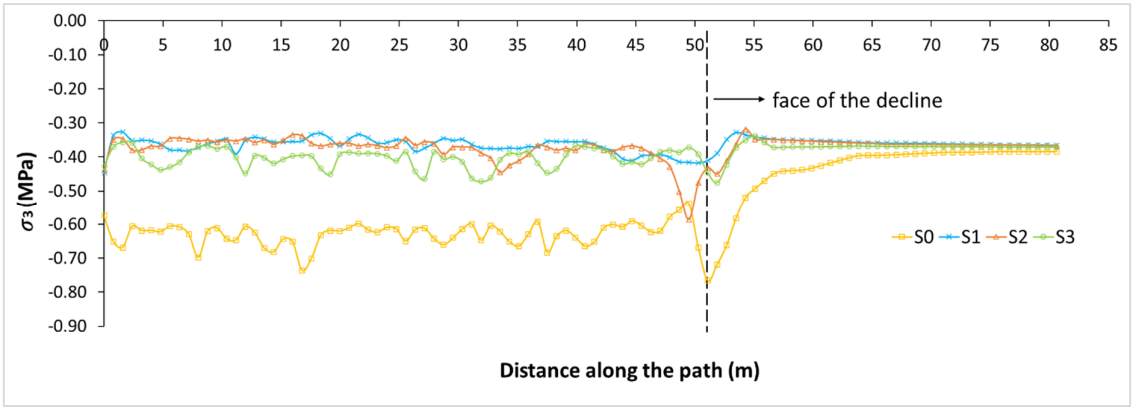

a) Distribution of minimum principal stresses.

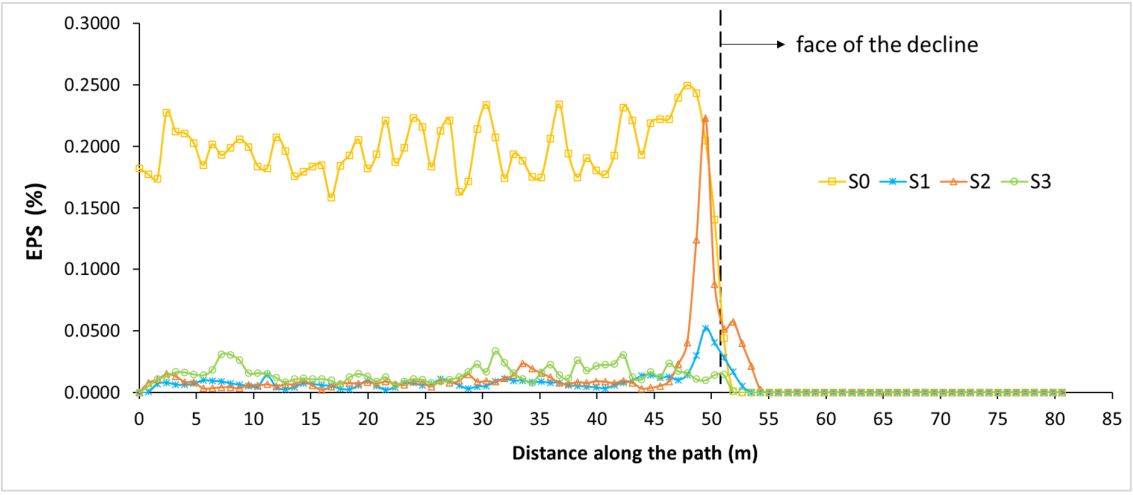

b) Distribution of equivalent plastic strain

Figure 18. Parameters recorded along path 1-2 for conditions S0, S1, S2, and S3.

Table 6. Comparison of the effect of conditions S0, S1, S2, and S3 on parameters.

Conditions	σ_3 (MPa)	EPS (%)
S0 and S3	0.8 MPa reduced (50%) to 0.4 MPa	0.10% reduced to almost 0.01% i.e. close to zero
S1 and S3	0.4 MPa for both models	Jumped to 0.025% from 0.01%
S1 and S2	0.4 MPa increased (5%) to 0.42 MPa	Jumped to 0.05% from 0.025%

6. Conclusions

The paper presents a solution to mine first 50 m of the two ore bodies MB and NB below the ultimate pit level underground below an open-pit mine composed of friable ore bodies and friable host rocks without leaving a crown pillar, and especially in a situation, where the traditional mining methods seemed precarious. A novel transverse Stopping method comprising of vertical long-hole blasting from the surface and mucking of ores from the underground is proposed. In order to ensure the possibility of the novel mining method on field, geotechnical studies comprising safe stope and pillar dimensions, sequence of mining and filling operations, support measures and slope stabilisation are performed, out of which slope stabilisation does not fall under the scope of the paper. At a time, only one stope will be mined and only after paste backfilling, the adjacent stope will be mined. The stope and pillar dimensions are decided after analysing the stope height among 30 m, 40 m, and 50 m, while the pillar width along the strike of the ore body is varied among 20 m, 40 m, and 60 m. A total of 36 models are analysed for considering different mining and filling sequences/operations. For each operation, a novel Mining Sequence Factor (MSF) is proposed, and estimated within a range of 0 and 1. This factor is an indicator of cumulative strength of 120 m of mining distance along the strike. The results from the models are extracted in terms of average value of equivalent plastic strain (AEPS) at 1 m below the UPL. A relationship between AEPS and MSF

suggests that in order to mine MB and NB ore bodies safely with transverse Stopping method, MSF must be more than 0.35 and AEPS below 8×10^{-4}. It, thus, is decided that at no point of time, pillar dimensions, either in situ or backfilled or both, should be less than 40 m. Further, a sensitivity analysis is performed that implies the mining method suggested in this paper is applicable even if material properties vary in the field.

Finally, the support system of the decline/drives to be constructed in limonitic rock must have the combination of RCC liner of 30 cm thickness and steel arches at 1 m distance. Based on the stresses and EPS distributions, it is concluded that the length of excavation that may be left unsupported from the face shall not exceed 1 m. The paper has attempted to provide a comprehensive solution to the unique and complex problem of extracting the friable ore bodies located beneath the open-pit mine hosted in friable rocks.

References

[1]. Soltani Khaboushan, A., & Osanloo, M. (2021). Determination of an optimum interface between open-pit and underground mining activities in Mazinu coal mine of Tabas power plant. *Journal of Mining and Environment*, *12*(1), 139-149.

[2]. Henning, J. G. (2007, May). Review of crown pillar investigations in a historic mine camp. In *ARMA Canada-US Rock Mechanics Symposium* (p. ARMA-07). ARMA.

[3]. Hutchinson, D. J., Phillips, C., & Cascante, G. (2002). Risk considerations for crown pillar stability assessment for mine closure planning. *Geotechnical & Geological Engineering*, *20*, 41-64.

[4]. Bakhtavar, E., Oraee, K., & Shahriar, K. (2010). Determination of the optimum crown pillar thickness between open-pit and block caving. In *29th International Conference on Ground Control in Mining* (pp. 325-332). Dept. of Mining Engineering, College of Engineering and Mineral Resources, West Virginia University.

[5]. Xu, S., Suorineni, F. T., An, L., Li, Y. H., & Jin, C. Y. (2019). Use of an artificial crown pillar in transition from open-pit to underground mining. *International Journal of Rock Mechanics and Mining Sciences*, *117*, 118-131.

[6]. Nicholas, D. E. (1981). Method selection-A numerical approach. *Design and operation of caving and sublevel Stopping mines*, 39-53.

[7]. Hartman, H.L. (1987). *Introductory Mining Engineering*, Wiley.

[8]. Dehghani, H., Siami, A., & Haghi, P. (2017). A new model for mining method selection based on grey and TODIM methods. *Journal of Mining and Environment*, *8*(1), 49-60.

[9]. Alpay, S., & Yavuz, M. (2007). A decision support system for underground mining method selection. In *New Trends in Applied Artificial Intelligence: 20th International Conference on Industrial, Engineering and Other Applications of Applied Intelligent Systems, IEA/AIE 2007, Kyoto, Japan, June 26-29, 2007. Proceedings 20* (pp. 334-343). Springer Berlin Heidelberg.

[10]. Karadogan, A., Bascetin, A., & Kahriman, A. (2001). A new approach in selection of underground mining method. *International Scientific Conference SGEM*. Bulgaria.

[11]. Karadogan, A., Kahriman, A., & Ozer., U. (2008). Application of fuzzy set theory in the selection of underground mining method. *Journal of the South African Institute of Mining & Metallurgy 108*(2), 73-79.

[12]. Yavuz, M., Iphar, M., & Once, G. (2008). The optimum support design selection by using AHP method for the main haulage road in WLC Tuncbilek colliery. *Tunnelling and Underground Space Technology*, *23*(2), 111-119.

[13]. Naghadehi, M. Z., Mikaeil, R., & Ataei, M. (2009). The application of fuzzy analytic hierarchy process (FAHP) approach to selection of optimum underground mining method for Jajarm Bauxite Mine, Iran. *Expert systems with applications*, *36*(4), 8218-8226.

[14]. Jamshidi, M., Ataei, M., Sereshki, F., & Jalali, S.M.E. (2009). The application of AHP approach to selection of optimum underground mining method, case study: Jajarm bauxite mine (Iran). *Archives of Mining Sciences 54*(1), 103-117.

[15]. Yavuz, M. (2015). The application of the analytic hierarchy process (AHP) and Yager's method in underground mining method selection problem. *International Journal of Mining, Reclamation and Environment, 29*(5), 453-475.

[16]. Zhao, X. D., Li, L. C., Tang, C. A., & Zhang, H. X. (2012). Stability of boundary pillars in transition from open pit to underground mining. *Journal of Central South University, 19*(11), 3256-3265.

[17]. Dintwe, T. K. M., Sasaoka, T., Shimada, H., Hamanaka, A., & Moses, D. (2022). Evaluating the influence of underground mining sequence under an open pit mine. *Journal of Mining Science, 58*(1), 35-43.

[18]. Phaisopha, S., Shimada, H., Sasaoka, T., Hamanaka, A., Pongpanya, P., Shorin, S., & Senthavisouk, K. (2023). A stope mining design with consideration of hanging wall when transitioning from open-pit mining to underground mining for Sepon gold mine deposit, Laos. *Mining, 3*(3), 463-482.

[19]. He, K., Swarbrick, G., & Sullivan, T. (2020). Numerical modelling of underground and open pit interaction in a gold mine. In *Proceedings of the 2020 International Symposium on Slope Stability in Open-Pit Mining and Civil Engineering* (pp. 1031-1046). Australian Centre for Geomechanics.

[20]. Bieniawski, Z. T. (1990). *Tunnel design by rock mass classifications*. Pennsylvania State University, Dept of Mineral Engineering.

[21]. NGI. 2022. *Using the Q-System, rock mass classification and support design*. NGI, Oslo, Norway.

[22]. Dalgic, S. (2000). The influence of weak rocks on excavation and support of the Beykoz Tunnel, Turkey. *Engineering geology*, *58*(2), 137-148.

[23]. Dalgic, S. (2002). Tunneling in squeezing rock, the Bolu tunnel, Anatolian Motorway, Turkey. *Engineering Geology*, *67*(1-2), 73-96.

[24]. Aygar, E. B. (2020). Evaluation of new Austrian tunnelling method applied to Bolu tunnel's weak rocks. *Journal of Rock Mechanics and Geotechnical Engineering, 12*(3), 541-556.

[25]. Opolony, K., Witthaus, H. (2003). Comparison of multiple- and single-entry roadway systems for highly stressed longwalls. In S. S. Peng, C. Mark, A. W. Khair, K. A. Heasley (Eds.), *Proceedings of the 22nd International Conference on Ground Control in Mining* (pp. 33-36). West Virginia University.

[26]. Witthaus, H., & Polysos, N. (2007). Rock mass classification in German hard-coal mining: standards and application. In *Proceedings of the International Workshop on Rock Mass Classification in Underground Mining*.

[27]. Palmstrom, A., & Stille, H. (2007). Ground behaviour and rock engineering tools for underground excavations. *Tunnelling and Underground Space Technology, 22*(4), 363-376.

[28]. Stille, H., & Palmström, A. (2008). Ground behaviour and rock mass composition in underground excavations. *Tunnelling and Underground Space Technology, 23*(1), 46-64.

[29]. Sanchez Fernandez, J. L., & Teran Benitez, C. E. (1994). Túnel de Trasvase Yacambú-Quibor: *Avance actual de los trabajos de excavación mediante la utilización de soportes flexibles aplicados a rocas con grandes deformaciones*. In *Proceedings of the IV Congreso Sudamericano de Mecanica de Rocas, Santiago 1*, 489-497.

[30]. Yan, P., Zhenguo, Z., Lu, W., Fan, Y., Chen, X., & Shan, Z. (2015). Mitigation of rock burst events by blasting techniques during deep-tunnel excavation. *Engineering Geology, 188*, 126-136. https://doi.org/10.1016/J.ENGGEO.2015.01.011

[31]. Cao, C., Shi, C., Lei, M., Yang, W., & Liu, J. (2018). Squeezing failure of tunnels: a case study. *Tunnelling and Underground Space Technology*, *77*, 188-203.

[32]. Marinos, V. (2014). Tunnel behaviour and support associated with the weak rock masses of flysch. *Journal of Rock Mechanics and Geotechnical Engineering, 6*(3), 227-239.

[33]. Hoek, E. (1998, November). Tunnel support in weak rock. In Keynote address, *Symposium of Sedimentary Rock Engineering*, Taipei, Taiwan.

[34]. Lee, S., & Tseng, D. (2011). Review and perspective of expressway tunnels in Taiwan, China. *Journal of Rock Mechanics and Geotechnical Engineering*, *3*, 385-397.

[35]. Hoek, E., Carranza-Torres, C., & Corkum, B. (2002). Hoek-Brown failure criterion-2002 edition. In *Proceedings of NARMS-Tac*, *1*(1), 267-273.

[36]. Drucker, D. C., & Prager, W. (1952). Soil mechanics and plastic analysis for limit design. *Quarterly of Applied Mathematics, 10*(2), 157-165.

[37]. Dondapati, G. K. (2023). *Evaluation of mechanical behaviour of polymeric skin support for mining applications using experimental and numerical modelling methods* (Doctoral Dissertation). IIT Kharagpur Institutional Dissertational Repository. http://www.idr.iitkgp.ac.in/xmlui/

[38]. Carrieri, G., Grasso, P., Mahtab, A., & Pelizza, S. (1991). Ten years of experience in the use of umbrella-arch for tunnelling. In *Proceedings of the SIG Conference on Soil and Rock Improvement, 1*, 99-111.

[39]. Bureau of Indian Standards. (2000). *IS 456: Code of practice for plain and reinforced concrete.* Bureau of Indian Standards.

ارزیابی پایداری عملیات توقف در اجسام سنگ شکن تحت یک معدن روباز با استفاده از فاکتور توالی استخراج مبتنی بر قدرت

سروتی ناروال[1*]، دباسیس دب[1]، سرنیواسا رائو اسلاوات[1]، و گوپینات سامانتا[2]

۱- گروه مهندسی معدن، موسسه فناوری هند، خاراگپور، هند

۲- تکنسین ارشد (معدن)، گروه فناوری فرآیند، تاتا استیل لیمیتد، جمشدپور، هند

ارسال ۲۰۲۴/۰۸/۰۲، پذیرش ۲۰۲۴/۱۲/۰۶

* نویسنده مسئول مکاتبات: srutinarwal27@gmail.com

چکیده:

یک روش جدید استخراج زیرزمینی برای استخراج سنگ معدن کرومیت شکننده در سنگ میزبان لیمونیتی ضعیف و هوازده در زیر یک معدن روباز پیشنهاد شده است. روش‌های مرسوم زیرزمینی اعتمادی را القا نمی‌کنند زیرا GSI (شاخص قدرت زمین‌شناسی) توده‌های سنگ و سنگ میزبان زیر ۳۵ قرار دارد. مجموعه‌ای از ابعاد توقف‌های عرضی در امتداد ضربه بر اساس تجزیه و تحلیل دقیق عملیات‌های معدنی و پس‌پر کردن چندگانه با شبیه‌سازی ۳۶ پیشنهاد شده‌اند. مدل های عددی سه بعدی برای هر عملیات یا توالی، یک "فاکتور توالی معدن (MSF)" مبتنی بر قدرت ابداع شده است که به تعیین کمیت قدرت معادل آن در مقایسه با شرایط درجا کمک می کند. این عامل همراه با میانگین کرنش پلاستیک معادل (AEPS) توسعه یافته بر روی ستون ها که از مدل های عددی به دست آمده است برای تعیین عملیات ایمن با هدف تولید سالانه مورد نظر استفاده می شود. این مقاله تجزیه و تحلیل عمیقی از این روش ارائه می‌کند و حداقل ابعاد ستون ۴۰ متر را، چه در محل و چه در محل، پیشنهاد می‌کند. این مقاله، علاوه بر این، طراحی درایوهای زیرزمینی و سیستم پشتیبانی آنها را طبق دستورالعمل‌های NGI (موسسه ژئوتکنیک نروژ) و مطالعات عددی سه‌بعدی ارائه می‌کند، که عملکرد آن با در نظر گرفتن توزیع تنش و کرنش پلاستیک معادل آن تحلیل می‌شود..

کلمات کلیدی: سنگ معدن و سنگ میزبان شکننده، استخراج زیر گودال روباز، روش جدید استخراج، سیستم استوپ و ستونی، فاکتور توالی معدن.